

A network-based mobile positioning system using an optimization model

Ahmad Sabri, Rifki Kosasih

Department of Informatics, Faculty of Computer Science and Information Technology, Gunadarma University, Depok, Indonesia

Article Info

Article history:

Received Nov 1, 2023

Revised Jan 16, 2024

Accepted Mar 6, 2024

Keywords:

Mobile positioning

Optimization

Prediction

Signal strength

Triangulation

ABSTRACT

The expansion of cellular network coverage facilitates the advancement of research on network-based positioning. We are interested in the signal fingerprinting method to predict the location of a mobile device. By this method, the device must be within the fingerprint coverage to have a successful location prediction. However, any disturbance in the signal propagation would decrease the prediction accuracy. We propose an optimization model based on generalized triangulation combined with a signal fingerprint which is treated more adaptively in responding to any signal disturbance. The triangulation method determines the most likely region where the device is located. The solution provides the estimated longitude and latitude of the device. An illustration of the implementation of the model is presented. The model is assessed using the Indosat cellular network in three distinct testbeds in Indonesia, which are: South Jakarta, a metropolitan area; South Tangerang, a buffer area adjacent to the metropolitan area; and Malang, a city surrounded by rural areas. The most favorable outcome yields an average prediction error of 39.6 m, a maximum error of 197.08 m, a minimum error of 0.05 m, and a standard deviation of error of 39.22 m.

This is an open access article under the [CC BY-SA](https://creativecommons.org/licenses/by-sa/4.0/) license.



Corresponding Author:

Rifki Kosasih

Department of Informatics, Faculty of Computer Science and Information Technology

Gunadarma University

Margonda Raya No. 100, Depok, 16424, Indonesia

Email: rifki_kosasih@staff.gunadarma.ac.id

1. INTRODUCTION

Network-based positioning is considered a viable alternative to satellite-based positioning methods, i.e., the global positioning system (GPS), for geolocation. The system makes use of the available attributes found in the network measurement report (NMR) of the surrounding base transceiver stations (BTSs or “towers”), i.e., reference signals received power (RSRP) in long-term evolution (LTE) networks or received signal strength indication (RSSI) in global system for mobile communications (GSM) networks. Previous research in [1] and [2] examines the variability in RSSI caused by shadowing effects. This research employs Bayes' rule to derive probability density functions that describe the distribution of propagation distances from all reported (i.e., serving and neighboring) cellular base stations. The location of the device is determined by combining probability density functions of involved cells, and Bayes' rule is used to find the most probable location. The field experiment yields a mean error of 52.8 meters, which is the distance from the actual position. Research by Liu *et al.* [3] examines the relationship between signal attenuation and RSSI using the Pearson correlation coefficient (PCC), as well as incorporating Bayes' rule. The location of the device is determined by the one having the highest PCC. The results of the test indicate that 80% of the mean error was under 300 m. Given the intricate relationship between signal strength and distance, some research

proposes the utilization of signal fingerprinting as an alternative to signal propagation models. The enhancement of fingerprint-based prediction techniques discussed in [4] considers the handover procedure dynamics between serving cell towers. Approximately 67% of the errors exhibit values that are lower than 124 m. Research by Ibrahim and Youssef [5] utilizes a combination of deterministic and probabilistic grid-based fingerprinting techniques, resulting in median errors of 105 m in rural and 30 m in urban areas, respectively. An infrastructure-free ubiquitous localization system is given in [6], giving median accuracies of 152 m in urban and 224 m in rural areas. The subsequent research employs the utilization of relative RSSI to estimate the geographical coordinates of a device in both urban and rural environments [7], revealing that the rural area exhibited a maximum error of 500 m, while the urban area displayed a maximum error of 400 m. Research by Meniem *et al.* [7] enhances the previous findings by incorporating the consideration of relative RSSI ordering, yielding a mean error of 29 m in urban areas and 55 m in rural areas. A technique of customized triangulating signal strength across three BTSs is proposed in [8].

Research by Kosasih and Sabri [9] employs a weighted centroid method that relies on signal strength. The estimated location of the device is given by the aggregated-cells centroid, which is obtained based on the weighted average of the BTSs coordinates. The weight of each BTS depends on its RSSI value. This approach can be implemented without the need to ascertain the potential overlap of signal strengths across each BTS [10]–[13]. Based on the findings, the maximum error recorded was 837.9511 meters, while the mean error was calculated to be 214.8366 meters. Nevertheless, the quantity of BTS identified by the device fluctuates along with the relocation of the device.

Improving the previous results, we employ a dynamic weighted centroid model that considers the variability in the number of BTSs reported in the nuclear magnetic resonance (NMR) [14]. We find that the cumulative distribution functions (CDFs) error of the dynamic weighted centroid model demonstrates a reduction of approximately 48.28% for errors under 100 m, 74.47% for errors under 150 m, 89.72% for errors under 200 m, and 97.81% for error under 250 m. Research by Ezema and Ani [15] employs a multi-linear regression model that relies on RSSI. The research yielded findings indicating that approximately 67% of positioning errors were below 64 m, and 95% of positioning errors were below 115 m. It was observed that the maximum error reached 275 m in urban areas. Nevertheless, the employed model exhibits a high degree of complexity.

In addition to employing RSSI, there exist research investigations that utilize time-based measurement techniques. The proposed signal attenuation method by Lin and Juang [16] demonstrates a mean error of 272.4 m in rural areas and 55 m in urban areas when considering time differences. Making use of timing advances in LTE networks, as discussed in [17], presents a theoretical opportunity to achieve a level of accuracy that is less than 0.5 meters. This method can be considered one of the most theoretically optimistic approaches based on network analysis. Nevertheless, there was no empirical assessment or experimental validation of this approach. As per the authors' assertions, the implementation during the specified period in 2011 remained limited because of the absence of adequate field-testing facilities that were compatible with a fully operational LTE network and testing equipment software.

According to Shakir *et al.* [18], it is found that activating timing advances in an established LTE network leads to an increase in network signaling load caused by multipath effects. With the current smartphone operating system, timing advance attributes are often unavailable. As alternatives, researchers examine the attributes of RSRP and PCI instead. The field tests yield a maximum error of 320 meters, as determined by optimal conditions.

It is noteworthy to mention several outcomes of indoor localization. In contrast to outdoor localization, indoor localization exhibits a narrower spatial coverage, albeit with a higher density of reference points. This methodology enables the generation of a fingerprint with enhanced resolution, thereby facilitating a more accurate estimation. The initial precise GSM indoor localization method, achieving a median accuracy of 5 meters in extensive multi-floor buildings, is presented in [19]. A more precise approach is proposed in [20] by employing vector similarity, resulting in an error margin of 0.4 m. See for more recent results in [21]–[23].

Common deterministic fingerprinting techniques for network-based localization store a vector representing the signal strength (RSSI, RSRP, or RSRQ) from a series of reported cell towers at the device location. According to Ibrahim and Youssef [5], to serve a location request, the vector of signal strength at an unknown location of the device is compared to the vectors recorded in the fingerprint by using the k-nearest neighbors (kNN) algorithm, in terms of signal strength space. The results are k-closest fingerprint locations, which are averaged as the estimated location. However, any actual disturbance in the signal propagation would make the situation deviate from the pre-recorded fingerprint. This could fail the method to predict the device location, even if it lies inside the coverage.

Our method proposes a combination of fingerprinting and triangulation optimization. This allows one to obtain the result even if there are signal propagation disturbances. The optimization model treats the fingerprint more adaptively in responding to any signal disturbance. Instead of calculating tower-to-device

distance by wave propagation models with shadowing terms, the fingerprint gives a more realistic tower-to-device distance that corresponds with the actual signal strength at the location of the device. The fingerprint's tower-to-device distance would then be used in the constraints of the triangulation optimization model, in which the towers act as reference points. Triangulation is employed to determine the most likely location of the device by utilizing the parameters obtained from the fingerprint. Our research gives two contributions: the first is to combine fingerprinting and triangulation methods to get more realistic tower-to-distance parameters, and the second is to get wider coverage beyond the fingerprint space.

This manuscript represents the expanded iteration of our concise paper that was delivered at the ACOMP 2021 conference [24]. The rest sections of the paper are as follows: in section 2, the construction and conceptual framework underlying the model as well as the detailed account of the methodology employed for constructing and implementing the model; section 3 provides a comprehensive analysis of the model's implementation and evaluation. Lastly, section 4 provides a concise conclusion of the findings.

2. RESEARCH METHOD

The triangulation formula is given by the simultaneous as (1):

$$\begin{cases} (x_L - x_P)^2 + (y_L - y_P)^2 = d_{PL}^2 \\ (x_M - x_P)^2 + (y_M - y_P)^2 = d_{PM}^2 \\ (x_N - x_P)^2 + (y_N - y_P)^2 = d_{PN}^2 \end{cases} \quad (1)$$

where L, M , and N are noncollinear points at known coordinates (x_L, y_L) , (x_M, y_M) , (x_N, y_N) , respectively, P is a point at an unknown coordinate (x_P, y_P) , and d_{PL} , d_{PM} , d_{PN} are known distances to P from L, M, N , respectively.

By the triangulation, the location of an object at an unknown position (x_P, y_P) is discoverable since the three reference points' coordinates and their distances to P are known. The object location is at the intersection point of three circles centered in L, M, N with a radius d_{PL} , d_{PM} and d_{PN} , respectively. In case d_{PL} , d_{PM} and d_{PN} exceeds the actual distance, then the object is located somewhere inside the intersection region of the three circles (see Figure 1). In this case, all the '=' relations in the triangulation formula are replaced by ' \leq '. We address this case as *loose triangulation*, and as *loose n-angulation* if it involves $n > 3$ reference points.

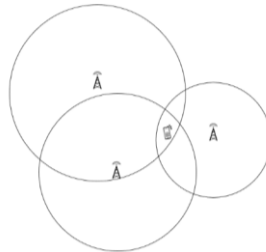


Figure 1. The case where the intersection of the three circles is a region instead of a point

On the surface of a great sphere (i.e., earth), the distance between point L at coordinate (x_L, y_L) and M at (x_M, y_M) , measured in radians, is given by the haversine formula (2) [25]–[27].

$$d_{LM} = 2r \sin^{-1} \left(\sqrt{\sin^2 \left(\frac{x_M - x_L}{2} \right) + \cos x_L \cos x_M \sin^2 \left(\frac{y_M - y_L}{2} \right)} \right) \quad (2)$$

where r is the earth's curvature radius (6,371 km).

For a small area on a round surface, with several kilometers (for instance, a small part of a city), the formula of equirectangular is used instead of haversine as (3):

$$d_{LM} = r \sqrt{\left((y_M - y_L) \cos \frac{x_M + x_L}{2} \right)^2 + (x_M - x_L)^2} \quad (3)$$

in (3) maps a round surface into a flat rectangular grid while maintaining size, shape, and area. Compared to harvesine for calculating small distances, the equirectangular formula gives a smaller relative mean of error [28].

To estimate the location of the device, we propose an optimization model whose parameters are determined by the current reported NMR and pre-developed fingerprint from up to seven reported cells from the covered area (collected through wardriving), constrained by general loose triangulation of the cells. The estimated location coordinate of the device is given by the solution of the model. The attributes recorded in the fingerprint are explained in Table 1.

Table 1. The attributes in the fingerprint and their meaning

Attribute	Explanation
c_i	Cell-ID (CID) of the i -th cell tower.
s_{c_i}	Signal strength that corresponds to c_i , measured in dBm.
$C_i = (x_i, y_i)$	The latitude x_i and longitude y_i of cell tower c_i in radians.
$L = (x_L, y_L)$	The latitude x_L and longitude y_L of the location where the device records the measurement, in radians. This location is the ground truth of the device's location by GPS.
d_{c_iL}	The distance from C_i (cell tower c_i) to L (device) in kilometers.

The following notions underlie the development of the prediction model.

Definition 1. Let $p = (p_1, p_2, \dots, p_n)$ and $q = (q_1, q_2, \dots, q_n)$ be vectors with distinct components.

- i. The *similarity* of vector p to vector q is the number of components of p that match the components of q .
- ii. If V is a set of vectors, then vector(s) in V that are *most similar* to q are those in V that have the largest similarity to q .

Definition 2. Let $p = (p_1, p_2, \dots, p_n)$ and $q = (q_1, q_2, \dots, q_n)$ be vectors with distinct components arranged in decreasing order. The *alignment vector* p to q , denoted by $a_{p,q} = (a_1, a_2, \dots, a_n)$, is a vector such that p_i matches with q_{a_i} , and $a_i = 0$ if p_i does not match any component of q .

Definition 3. Given alignment vector $a_{p,q} = (a_1, a_2, \dots, a_n)$. The *matching vector* $m_{p,q} = (m_1, m_2, \dots, m_n)$ is a vector where $m_i = 0$ if $a_i = 0$, and $m_i = 1$ if $a_i \neq 0$.

Definition 4. Given vectors $p = (p_1, \dots, p_n)$ $q = (q_1, q_2, \dots, q_n)$, with alignment vector $a_{p,q} = (a_1, a_2, \dots, a_n)$. The *closeness* between vector p and q based on vector a is defined as (4):

$$\kappa_{p,q} = \sum_{i=1}^n m_i |q_{a_i} - p_i| \tag{4}$$

where m_i is the i -th element of matching vector m .

Vector $c_A = (c_{A1}, c_{A2}, \dots, c_{A7})$ is a vector of reported CIDs at an unknown location A , arranged in decreasing order; vector $s_A = (s_{c_{A1}}, s_{c_{A2}}, \dots, s_{c_{A7}})$ is a vector of reported signal strengths that correspond to c_{Ai} . If there is no reported CID and signal strength from the i -th cell, then $c_{Ai} = s_{c_{Ai}} = 0$. The set F is defined as the collection of rows in the fingerprint, which contains:

- i. Row vector of CIDs (possibly there were multiple rows) that are most similar to c_A (denoted by $c_F = (c_{F1}, c_{F2}, \dots, c_{F7})$), and
- ii. Row vectors of signal strength denoted by $s_F(i)$, where i is the row number in F .

For a given vector of CIDs c_F , the vector $C_F = ((x_{c_{F1}}, y_{c_{F1}}), (x_{c_{F2}}, y_{c_{F2}}), \dots, (x_{c_{F7}}, y_{c_{F7}}))$ provides the coordinates of the location of the cell $c_{F1}, c_{F2}, \dots, c_{F7}$, respectively.

Definition 5. Let d_{c_iL} be the values of the tower-to-device distance column in the fingerprint, and R be the set of some rows of d_{c_iL} . Then (5).

$$D_i = \max(d_{c_iL} | R) \tag{5}$$

In other words, D_i is the maximum value in d_{c_iL} column of all rows in R .

Definition 6. Given c_A and c_F vectors of the length n , where c_i the i -th component of c_A . Let $a_{c_A, c_F} = (a_1, a_2, \dots, a_n)$ be the alignment vector of c_A and c_F . The notion (6):

$$\delta_i = D_{a_i} \tag{6}$$

denotes the fingerprint's maximum tower-to-device distance of the tower having CID c_i .

For a given c_A (the vector of reported cell-IDs) and s_A (the vector of signal strengths of the reported cells), the values of the following parameters are assigned from the fingerprint: i) c_F (the most similar vector to c_A), ii) C_F (the vector containing the latitude and longitude of each cell in c_F), iii) a_{c_A,c_F} (the alignment vector), and iv) m_{c_A,c_F} (the matching vector).

Next is to define our triangulation optimization model. The solution is the prediction of device location. Let P be the predicted location of the device with latitude x_P and longitude y_P in radians, C_iP be the vector that begins at C_i and ends at P , d_{C_iP} be the distance from C_i to P . The dynamic triangulation model is defined as (7).

$$\begin{aligned}
 & \max |m_1C_1P + m_2C_2P + \dots + m_7C_7P| \\
 & \text{Subject to:} \\
 & (1) d_{C_1P} \leq \delta_1, \\
 & (2) d_{C_2P} \leq \delta_2, \\
 & \quad \vdots \\
 & (7) d_{C_7P} \leq \delta_7,
 \end{aligned}
 \left. \vphantom{\begin{aligned} \max \\ \text{Subject to:} \end{aligned}} \right\} (7)$$

$$\text{where } d_{C_iP} = 6371 \sqrt{\left((y_P - y_{C_i}) \cos \frac{x_{C_i} + x_P}{2} \right)^2 + (x_P - x_{C_i})^2},$$

$$\begin{aligned}
 & x_P, y_P \text{ unbounded,} \\
 & \text{constraint } i \text{ is added if } m_i = 1
 \end{aligned}$$

The objective function is to find the location P such that the absolute of the summation of vectors PC_i is maximum. See Figure 2 for an illustration of these vectors, restricted to four cells' involvement.

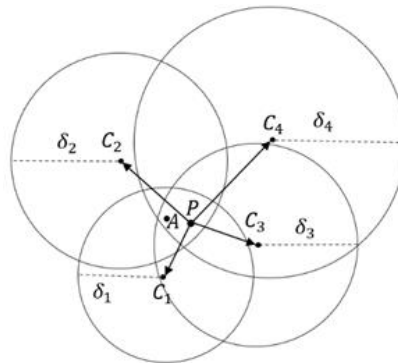


Figure 2. Predicted position P and actual position A . Location P is determined such that the absolute of the summation of vectors PC_i is maximum

The prediction error d_{AP} is determined by the distance between the actual position (x_A, y_A) and predicted position (x_P, y_P) . It is calculated by (3). Our method consists of two stages: development and implementation. In brief, the development stage is to develop the system by creating the signal fingerprint and client/server-side codes. The fingerprint is collected by wardriving to record c_i , s_{c_i} , C_i , L and d_{c_iL} attributes (explained previously in Table 1). The wardriving records NMR of up to seven cells per second. Typical our fingerprint is shown partially in Table 2. The table shows grouped consecutive columns c_i, s_{c_i}, d_{c_iL} , that record CID, signal strength, and tower-to-device distance, respectively, while the device's position is at (lat_A, lon_A) as shown by the two rightmost columns. Each row records NMR for every second of wardriving. The implementation stage is to put the developed system into action. At this stage, the client sends a request for location service to the server, and the server responds by solving the optimization model based on the NMR sent from the client, and finally sending the result (i.e., the estimated location) to the device.

Table 2. The sample of rows in the fingerprint

c_1	s_{c_1}	d_{c_1L}	c_2	s_{c_2}	d_{c_2L}	c_3	s_{c_3}	d_{c_3L}	c_4	s_{c_4}	d_{c_4L}	c_5	s_{c_5}	d_{c_5L}	c_6	s_{c_6}	d_{c_6L}	c_7	s_{c_7}	d_{c_7L}	lat_A	lon_A	
:	:	:	:	:	:	:	:	:	:	:	:	:	:	:	:	:	:	:	:	:	:	:	:
62493-710.393762491-790.938034501-770.093020801-810.635617633-790.619117632-750.287017631-510.2439-6.2835106.7305																							
62493-710.395562491-790.936934501-770.091920801-810.635617633-790.617417632-750.288617631-510.2417-6.2835106.7305																							
62493-710.405562491-790.928934501-790.090720801-810.632117633-810.607517632-770.298117631-590.2313-6.2835106.7306																							
62493-710.407162491-790.927434501-790.091420801-810.631017633-810.605917632-770.299717631-590.2300-6.2834106.7306																							
62493-710.408062491-790.926834501-810.091020801-810.631017633-810.605117632-770.300517631-570.2289-6.2834106.7306																							
62493-710.409262491-790.926734501-810.089220801-810.632117633-810.604017632-770.301417631-570.2270-6.2835106.7306																							
62493-730.415362491-790.922434501-810.088320801-830.631117633-830.598117632-770.307117631-570.2202-6.2834106.7307																							
62493-730.416562491-790.922234501-810.086720801-830.632217633-830.597117632-770.308117631-570.2183-6.2835106.7307																							
:	:	:	:	:	:	:	:	:	:	:	:	:	:	:	:	:	:	:	:	:	:	:	:

To construct the model based on NMR sent by the device, the following parameters need to be acquired in advance: i) $C_i = (x_i, y_i)$, the latitude and longitude of the i -th cell tower, ii) δ_i , the estimated distance to the device from the i -th cell tower, and iii) m_i , a boolean value, where $m_i = 1$ if the i -th cell tower is not null, $m_i = 0$ otherwise (i.e., to include constraint i in the model if $m_i = 1$, or otherwise if $m_i = 0$).

The parameter C_i , is assigned directly from the fingerprint with a simple look-up command based on CID c_i . A special procedure is needed to obtain the values of the parameters δ_i and m_i . For an input vector of reported CIDs $c_A = (c_{A1}, c_{A2}, \dots, c_{A7})$ and the vector of its corresponding signal strength $s_A = (s_{A1}, s_{A2}, \dots, s_{A7})$, the procedure looks up for the set of rows R having a vector $c_F = (c_{F1}, c_{F2}, \dots, c_{F7})$ that is most similar to c_A (by definition 1), along with c_F 's corresponding vector of signal strength $s_F = (s_{F1}, s_{F2}, \dots, s_{F7})$ that is the closest to s_A (by definition 4). From the rows in R , we obtain D_1, D_2, \dots, D_7 (by definition 5), the maximum tower-to-device distance of each cell. The maximum values are chosen so that the circles of cells intersect, creating a region in which the device is possibly located. From this set of D_i , we obtain δ_i (by definition 6) based on the alignment vector a_{c_A, c_F} (by definition 2) and its matching vector m_{c_A, c_F} (by definition 3).

In the implementation stage, the request for location service is performed by the device. The server received c_A, s_A sent through an internet connection from the device at the unknown location A . At the server, the system looks for the fingerprint for $c_F, C_F, a_{c_A, c_F}, m_{c_A, c_F}$ that correspond to c_A and s_A . If success, then it assigns a value to each δ_i , followed by passing C_i, δ_i, m_i to the model expressed by the optimization model in (7). The system then solves the model, and the result (which is the estimated latitude/longitude of the device), is transferred back to the device. In the following, we summarize the procedure for developing a network-based positioning system. Figure 3 gives the method schematically.

- a. Stage 1: development
 - i. Create a raw NMR fingerprint of the desired area by wardriving.
 - ii. Preprocessing: for each row of the fingerprint, sort the NMR of each tower by CID in descending order. The NMR with a larger CID number comes to the left of the smaller ones.
 - iii. Referring to the cell tower database, calculate the tower-to-device distance by using (3).
 - iv. Upload the fingerprint to a cloud database server.
 - v. Create a server-side code to receive location requests and NMR sent from the client, to look up the appropriate fingerprint instances based on received NMR, and to solve the model whose parameters correspond to the current NMR and appropriate fingerprint instances.
- b. Stage 2: implementation (serving location request from the client device)
 - i. The client sends location requests by sending its current NMR c_A and s_A to the server by internet connection.
 - ii. The server-side code looks up the fingerprint for c_F , the CID vectors that most similar to c_A . This look-up procedure produces an alignment vector a_{c_A, c_F} and matching vector m_{c_A, c_F} .
 - iii. Among these most similar vectors c_F , find those having s_F the closest to s_A (based on alignment vector a_{c_A, c_F}).
 - iv. Among the closest vectors within c_F , get the furthest tower-to-device distance δ_i for each CID (based on alignment vector a_{c_A, c_F}).
 - v. Construct optimization model by parameters given by vector C_F (containing the coordinates of the cell towers), m_{c_A, c_F} , and δ_i .
 - vi. Solve the model to get the estimated location (the coordinates) of the device.
 - vii. Send back the result to the client.

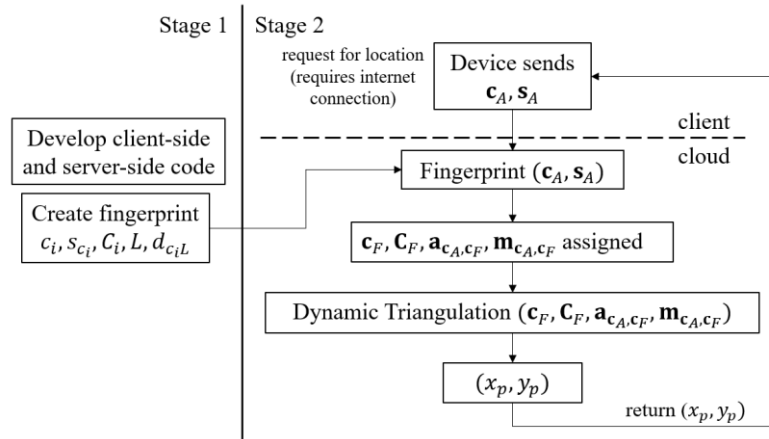


Figure 3. Methodology

3. RESULTS AND DISCUSSION

This section begins with providing an instance in the implementation stage and evaluation of the performance. The fingerprint, the instance, and the evaluation are created and performed within the Indosat cellular network, a major service provider in Indonesia. The implementation in other cellular network providers is made possible by creating the appropriate fingerprint of the network.

3.1. An instance of location service request

Suppose a device requests a geolocation and sends the following NMR to the system:

$$c_A = (62493, 34501, 20801, 17633, 17632, 17631, 0),$$

$$s_A = (-73, -83, -85, -85, -69, -57, 0)$$

A fingerprint has already been built previously, and it covers the area where the device sends the request. Figure 4 shows the construction of c_F from the part of the fingerprint having the vector that most similar to c_A . We refer to these rows as the set F . At this point we have

$$c_F = (62493, 62491, 34501, 20801, 17633, 17632, 17631)$$

Vector c_F has 6 similar CIDs to c_A , except the second element 62,491. By definition 2, the alignment vector c_A to c_F is $a_{c_A, c_F} = (1, 3, 4, 5, 6, 7, 0)$. Figure 5 shows the steps to obtain a_{c_A, c_F} from vectors c_A and c_F .

c_1	s_{c_1}	d_{c_1L}	c_2	s_{c_2}	d_{c_2L}	c_3	s_{c_3}	d_{c_3L}	c_4	s_{c_4}	d_{c_4L}	c_5	s_{c_5}	d_{c_5L}	c_6	s_{c_6}	d_{c_6L}	c_7	s_{c_7}	d_{c_7L}	lat_A	lon_A
62493	-71	0.39365	62491	-79	0.93799	34501	-77	0.09296	20801	-81	0.63562	17633	-79	0.61914	17632	-75	0.28696	17631	-51	0.24387	-6.2835	106.7305
62493	-71	0.39545	62491	-79	0.93685	34501	-77	0.09190	20801	-81	0.63557	17633	-79	0.61739	17632	-75	0.28857	17631	-51	0.24170	-6.2835	106.7305
62493	-71	0.40552	62491	-79	0.92890	34501	-79	0.09073	20801	-81	0.63212	17633	-81	0.60747	17632	-77	0.29813	17631	-59	0.23130	-6.2835	106.7306
62493	-71	0.40706	62491	-79	0.92738	34501	-79	0.09136	20801	-81	0.63100	17633	-81	0.60592	17632	-77	0.29970	17631	-59	0.23000	-6.2834	106.7306
62493	-71	0.40797	62491	-79	0.92682	34501	-81	0.09098	20801	-81	0.63100	17633	-81	0.60505	17632	-77	0.30051	17631	-57	0.22892	-6.2834	106.7306
62493	-71	0.40916	62491	-79	0.92666	34501	-81	0.08919	20801	-81	0.63211	17633	-81	0.60399	17632	-77	0.30141	17631	-57	0.22696	-6.2835	106.7306
62493	-73	0.41528	62491	-79	0.92238	34501	-81	0.08833	20801	-83	0.63105	17633	-83	0.59809	17632	-77	0.30711	17631	-57	0.22024	-6.2834	106.7307
62493	-73	0.41650	62491	-79	0.92224	34501	-81	0.08671	20801	-83	0.63220	17633	-83	0.59705	17632	-77	0.30805	17631	-57	0.21829	-6.2835	106.7307

$c_F = (62493, 62491, 34501, 20801, 17633, 17632, 17631)$

Figure 4. Constructing c_F from the fingerprint. The collection of all rows in this part is referred to as F

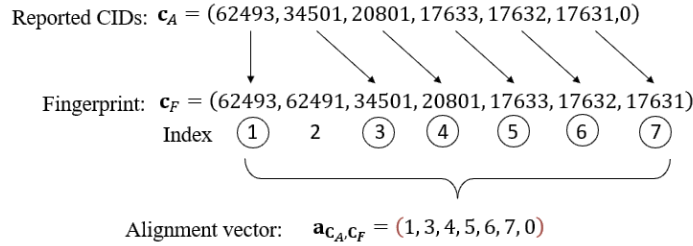


Figure 5. Assigning value to the vector $\mathbf{a}_{\mathbf{c}_A, \mathbf{c}_F}$

From the fingerprint, we have the following vectors of signal strength $\mathbf{s}_F(j) = (s_{F1}(j), s_{F2}(j), \dots, s_{F7}(j))$, where j is the relative row number in F .

- $\mathbf{s}_F(1) = (-71, -79, -77, -81, -79, -75, -51)$,
- $\mathbf{s}_F(2) = (-71, -79, -77, -81, -79, -75, -51)$,
- $\mathbf{s}_F(3) = (-71, -79, -79, -81, -81, -77, -59)$,
- $\mathbf{s}_F(4) = (-71, -79, -79, -81, -81, -77, -59)$,
- $\mathbf{s}_F(5) = (-71, -79, -81, -81, -81, -77, -57)$,
- $\mathbf{s}_F(6) = (-71, -79, -81, -81, -81, -77, -57)$,
- $\mathbf{s}_F(7) = (-73, -79, -81, -83, -83, -77, -57)$,
- $\mathbf{s}_F(8) = (-73, -79, -81, -83, -83, -77, -57)$.

The assignment of $\mathbf{s}_F(j)$ above is explained in Figure 6.

c_1	s_{e_1}	d_{c_1L}	c_2	s_{e_2}	d_{c_2L}	c_3	s_{e_3}	d_{c_3L}	c_4	s_{e_4}	d_{c_4L}	c_5	s_{e_5}	d_{c_5L}	c_6	s_{e_6}	d_{c_6L}	c_7	s_{e_7}	d_{c_7L}	lat_A	lon_A
62493	-71	0.39365	62491	-79	0.93799	34501	-77	0.09296	20801	-81	0.63562	17633	-79	0.61914	17632	-75	0.28696	17631	-51	0.24387	-6.2835	106.7305
62493	-71	0.39545	62491	-79	0.93685	34501	-77	0.09190	20801	-81	0.63557	17633	-79	0.61739	17632	-75	0.28857	17631	-51	0.24170	-6.2835	106.7305
62493	-71	0.40552	62491	-79	0.92890	34501	-79	0.09073	20801	-81	0.63212	17633	-81	0.60747	17632	-77	0.29813	17631	-59	0.23130	-6.2835	106.7306
62493	-71	0.40706	62491	-79	0.92738	34501	-79	0.09136	20801	-81	0.63100	17633	-81	0.60592	17632	-77	0.29970	17631	-59	0.23000	-6.2834	106.7306
62493	-71	0.40797	62491	-79	0.92682	34501	-81	0.09098	20801	-81	0.63100	17633	-81	0.60505	17632	-77	0.30051	17631	-57	0.22892	-6.2834	106.7306
62493	-71	0.40916	62491	-79	0.92666	34501	-81	0.08919	20801	-81	0.63211	17633	-81	0.60399	17632	-77	0.30141	17631	-57	0.22696	-6.2835	106.7306
62493	-73	0.41528	62491	-79	0.92238	34501	-81	0.08833	20801	-83	0.63105	17633	-83	0.59809	17632	-77	0.30711	17631	-57	0.22024	-6.2834	106.7307
62493	-73	0.41650	62491	-79	0.92224	34501	-81	0.08671	20801	-83	0.63220	17633	-83	0.59705	17632	-77	0.30805	17631	-57	0.21829	-6.2835	106.7307

$\mathbf{s}_F(1) =$	[-71	-79	-77	-81	-79	-75	-51]
$\mathbf{s}_F(2) =$	[-71	-79	-77	-81	-79	-75	-51]
$\mathbf{s}_F(3) =$	[-71	-79	-79	-81	-81	-77	-59]
$\mathbf{s}_F(4) =$	[-71	-79	-79	-81	-81	-77	-59]
$\mathbf{s}_F(5) =$	[-71	-79	-81	-81	-81	-77	-57]
$\mathbf{s}_F(6) =$	[-71	-79	-81	-81	-81	-77	-57]
$\mathbf{s}_F(7) =$	[-73	-79	-81	-83	-83	-77	-57]
$\mathbf{s}_F(8) =$	[-73	-79	-81	-83	-83	-77	-57]

Figure 6. The part of the fingerprint containing \mathbf{c}_F and the formation of $\mathbf{s}_F(j), j = 1, 2, \dots, 8$

The next step is to calculate $\kappa_{S_A, s_{F(i)}}$, the closeness between S_A to each $s_{F(i)}$ (by definition 4). The closeness is calculated based on $\mathbf{a} = \mathbf{a}_{\mathbf{c}_A, \mathbf{c}_F} = (1, 3, 4, 5, 6, 7, 0)$, and the corresponding matching vector $\mathbf{m}_{\mathbf{c}_A, \mathbf{c}_F} = (1, 1, 1, 1, 1, 1, 0)$. The closeness $\kappa_{S_A, s_{F(i)}}$ is obtained by (8).

$$\kappa_{S_A, s_{F(j)}} = \sum_{i=1}^7 m_i |s_{F a_j(j)} - s_{A i}| \tag{8}$$

For example, to calculate $\kappa_{S_A, s_{F(1)}}$,

$$\kappa_{S_A, s_{F(1)}} = m_1 |s_{F1}(1) - s_{A1}| + m_2 |s_{F3}(1) - s_{A2}| + m_3 |s_{F4}(1) - s_{A3}| + m_4 |s_{F5}(1) - s_{A4}| + m_5 |s_{F6}(1) - s_{A5}| + m_6 |s_{F7}(1) - s_{A6}| + m_7 |s_{F0}(1) - s_{A7}|$$

The last term becomes zero since $m_7 = 0$. For convenience, $s_{F0}(i) = 0$ for all i . It follows that

$$\kappa_{s_A, s_F(1)} = |-71 + 73| + |-77 + 83| + |-81 + 85| + |-79 + 85| + |-75 + 69| + |-51 + 57| = 30$$

By a similar calculation, we have:

$$\begin{aligned} \kappa_{s_A, s_F(2)} &= 30, \\ \kappa_{s_A, s_F(3)} &= \kappa_{s_A, s_F(4)} = 24, \\ \kappa_{s_A, s_F(5)} &= \kappa_{s_A, s_F(6)} = 20, \\ \kappa_{s_A, s_F(7)} &= \kappa_{s_A, s_F(8)} = 14. \end{aligned}$$

The results show that $s_F(7)$ and $s_F(8)$ have the least closeness to s_A . Next is to obtain the furthest tower-to-device distance from the rows that contain $s_F(7)$ and $s_F(8)$. Let $R \subset F$ be the set of rows in F that contains $s_F(7)$ and $s_F(8)$. In this case, R is the 7th and 8th rows of F (see Figure 7). The furthest tower-to-device distance is obtained by applying definition 5 on R as:

$$\begin{aligned} D_1 &= \max(d_{c_1L} | R) = \max(0.41528, 0.41650) = 0.4165, \\ D_2 &= \max(d_{c_2L} | R) = \max(0.92238, 0.92224) = 0.92238, \\ D_3 &= \max(d_{c_3L} | R) = \max(0.08833, 0.08671) = 0.08833, \\ D_4 &= \max(d_{c_4L} | R) = \max(0.63105, 0.63220) = 0.63220, \\ D_5 &= \max(d_{c_5L} | R) = \max(0.59809, 0.59705) = 0.59809, \\ D_6 &= \max(d_{c_6L} | R) = \max(0.30711, 0.30805) = 0.30805, \\ D_7 &= \max(d_{c_7L} | R) = \max(0.22024, 0.21829) = 0.22024. \end{aligned}$$

The assignment of D_i is explained in Figure 7.

c_1	s_{e_1}	d_{c_1L}	c_2	s_{e_2}	d_{c_2L}	c_3	s_{e_3}	d_{c_3L}	c_4	s_{e_4}	d_{c_4L}	c_5	s_{e_5}	d_{c_5L}	c_6	s_{e_6}	d_{c_6L}	c_7	s_{e_7}	d_{c_7L}	lat_A	lon_A
62493	-71	0.39365	62491	-79	0.93799	34501	-77	0.09296	20801	-81	0.63562	17633	-79	0.61914	17632	-75	0.28696	17631	-51	0.24387	-6.2835	106.7305
62493	-71	0.39545	62491	-79	0.93685	34501	-77	0.09190	20801	-81	0.63557	17633	-79	0.61739	17632	-75	0.28857	17631	-51	0.24170	-6.2835	106.7305
62493	-71	0.40552	62491	-79	0.92890	34501	-79	0.09073	20801	-81	0.63212	17633	-81	0.60747	17632	-77	0.29813	17631	-59	0.23130	-6.2835	106.7306
62493	-71	0.40706	62491	-79	0.92738	34501	-79	0.09136	20801	-81	0.63100	17633	-81	0.60592	17632	-77	0.29970	17631	-59	0.23000	-6.2834	106.7306
62493	-71	0.40797	62491	-79	0.92682	34501	-81	0.09098	20801	-81	0.63100	17633	-81	0.60505	17632	-77	0.30051	17631	-57	0.22892	-6.2834	106.7306
62493	-71	0.40916	62491	-79	0.92666	34501	-81	0.08919	20801	-81	0.63211	17633	-81	0.60399	17632	-77	0.30141	17631	-57	0.22696	-6.2835	106.7306
62493	-73	0.41528	62491	-79	0.92238	34501	-81	0.08833	20801	-83	0.63105	17633	-83	0.59809	17632	-77	0.30711	17631	-57	0.22024	-6.2834	106.7307
62493	-73	0.41650	62491	-79	0.92224	34501	-81	0.08671	20801	-83	0.63220	17633	-83	0.59705	17632	-77	0.30805	17631	-57	0.21829	-6.2835	106.7307

$\max \downarrow$ $\max \downarrow$ $\max \downarrow$ $\max \downarrow$ $\max \downarrow$ $\max \downarrow$ $\max \downarrow$

$D_1 = 0.41650$ $D_2 = 0.92238$ $D_3 = 0.08833$ $D_4 = 0.63220$ $D_5 = 0.59809$ $D_6 = 0.30805$ $D_7 = 0.22024$

Figure 7. The assignment of D_i from the fingerprint

D_i is the furthest-recorded distance from tower i to the device. Then by definition 6, we assign δ_i to D_{a_i} , where a_i is the i -th element of the alignment vector $a_{C_A, C_F} = (1, 3, 4, 5, 6, 7, 0)$:

$$\begin{aligned} \delta_1 &= D_{a_1} = D_1 = 0.4165, \\ \delta_2 &= D_{a_2} = D_3 = 0.08833, \\ \delta_3 &= D_{a_3} = D_4 = 0.63220, \\ \delta_4 &= D_{a_4} = D_5 = 0.59809, \\ \delta_5 &= D_{a_5} = D_6 = 0.30805, \\ \delta_6 &= D_{a_6} = D_7 = 0.22024. \end{aligned}$$

Recall the matching vector which corresponds to $a_{C_A, C_F} = (1, 3, 4, 5, 6, 7, 0)$ is $m_{C_A, C_F} = (1, 1, 1, 1, 1, 1, 0)$. This vector indicates that the prediction model includes the first to the sixth constraint. By dynamic triangulation model (7), the optimization model of this instance is given by (9):

$$\max |C_1P + C_2P + \dots + C_6P| \tag{9}$$

Subject to:

$$d_{C_1P} \leq \delta_1 = 0.41650$$

$$d_{C_2P} \leq \delta_3 = 0.08833$$

$$d_{C_3P} \leq \delta_4 = 0.63220$$

$$d_{C_4P} \leq \delta_5 = 0.59809$$

$$d_{C_5P} \leq \delta_6 = 0.30805$$

$$d_{C_6P} \leq \delta_7 = 0.22024$$

where $d_{C_iP} = 6371 \sqrt{\left((y_P - y_{C_i}) \cos \frac{x_{C_i} + x_P}{2} \right)^2 + (x_P - x_{C_i})^2}$,

x_P, y_P unbounded.

The i -th cell tower location coordinates (x_{C_i}, y_{C_i}) is acquired from the tower database. Solving this optimization yields x_P and y_P in radians, which is dedicated to the estimated location of the device.

3.2. Evaluation

The accuracy of the model is measured by the prediction error, which is the distance between the actual position and the predicted position. We test the model in three testbeds: South Jakarta, a typical metropolitan city having buildings and dense BTSs; South Tangerang, a buffer city of Jakarta, having less dense BTSs and is less crowded than South Jakarta; and Malang city, a medium-sized city surrounded with rural areas, having BTSs placed more distantly to each other. The recapitulation of the test results for each testbed is given in Tables 3 to 5, respectively. The prediction errors are evaluated in terms of average, maximum, minimum, and standard deviation, and categorize them based on the number of reported BTSs (from 3 to 7 and aggregate of all). Normally, fewer BTSs are reported if the device is surrounded by obstacles or situated in a less dense BTSs area. The “count” row measures the number of occurrences in the test. The test results give insight into how those metrics are affected by the number of reported BTSs. The metrics for aggregate are obtained by considering all numbers of reported BTSs. We will later in this section discuss the results by looking at the graph.

Table 3. Prediction error in South Jakarta (in meters)

Measurements	Reported BTSs					Aggregate
	3	4	5	6	7	
average	161.43	120.86	114.23	83.79	72.16	105.12
max	353.34	328.40	286.57	285.74	197.08	353.03
min	25.28	3.21	2.23	2.09	0.66	0.66
st. dev	125.65	81.14	63.29	60.56	56.77	73.65
count	82	270	567	443	139	1501

Table 4. Prediction error in South Tangerang (in meters)

Measurements	Reported BTSs					Aggregate
	3	4	5	6	7	
average	362.63	156.68	128.35	80.31	39.60	144.83
max	692.11	632.64	389.94	409.04	235.76	692.11
min	45.03	0.05	0.98	2.33	2.43	0.05
stdev	190.89	129.98	101.20	77.25	39.22	143.19
count	149	446	402	303	94	1394

Table 5. Prediction error in Malang (in meters)

Measurements	Reported BTSs					Aggregate
	3	4	5	6	7	
average	221.97	131.97	118.27	65.02	61.28	136.03
max	906.48	644.68	391.95	266.52	212.66	906.48
min	3.32	3.20	0.99	2.11	0.96	0.96
stdev	182.43	130.44	102.56	50.84	55.36	138.95
count	312	237	349	218	62	1178

Figure 8 shows the CDF of errors, the CDFs of error in our three testbeds are given in Figures 8(a) to 8(c). They are presented based on the number of reported towers BTSs. In general, the CDFs tend to skew

more to the left for a higher number of reported towers, which means better accuracy. An interesting finding is shown by the CDFs of 3 towers in all testbeds, which deviates significantly to the far right from the rest CDFs. This phenomenon is caused by the area of the cell intersection being too large. Our test reveals that the largest prediction error of the model in each testbed is given by the three towers' involvement (see again Tables 3 to 5). On the contrary, the best accuracy is generally given by 7 towers involvement. The best of our test is shown by CDF of 7 towers for South Tangerang, see Figure 8(b), which gives 91.49% of prediction error being less than 80 m with an error average of 39.60 m and a standard deviation of 39.22 m.

The aggregate results (joined 3 to 7 towers) are shown in Figure 8(d). The best results are given by the aggregate CDF of South Jakarta, with 90.85% of prediction errors being less than 200 m. Almost similar CDFs are given by South Tangerang and Malang, with 90.60% of prediction errors being less than 350 m (South Tangerang), and 89.45% of prediction errors being less than 360 m (Malang). We find also that the CDFs of the aggregates are close to the CDFs of 5 towers of their respective testbeds.

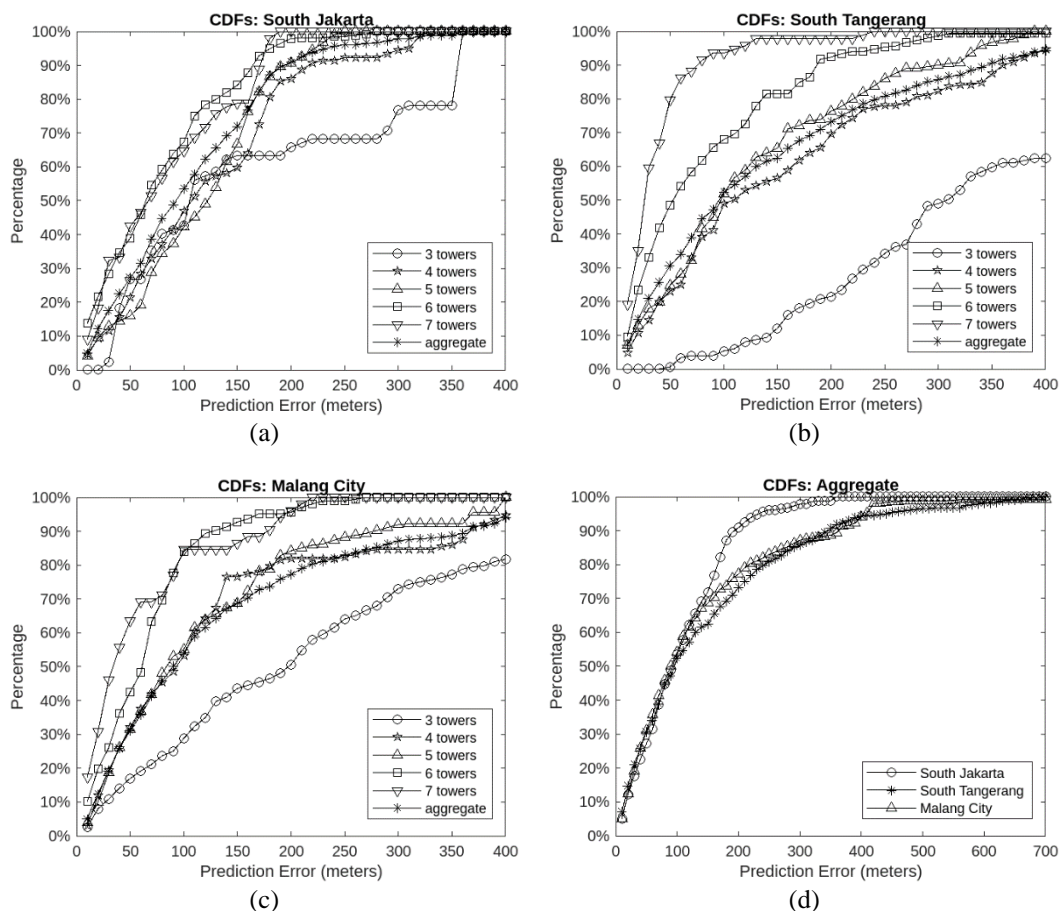


Figure 8. CDF of errors In (a) South Jakarta, (b) South Tangerang, (c) Malang, and (d) the aggregate

Figure 9 shows a range of errors concerning the number of reported towers. Among all testbeds, South Jakarta gives a more stable range of prediction errors for any number of reported towers. This is shown by the graph in Figure 9(a), where the minimum, average, and maximum lines tend to be horizontal, compared to Figure 9(b) (South Tangerang) and Figure 9(c) (Malang), which give more steep maximum and average lines. However, the minimum lines in the three testbeds tend to be stable and close to zero. Overall, the results propose that the accuracy is more stable in the region having more dense BTSs.

In terms of standard deviation, the trend is decreasing concerning the number of reported towers. It means that the prediction errors are distributed more closely around their respective average as the number of reported towers increases. The graph in Figure 9(d) shows this phenomenon. An interesting result is that the standard deviation line for South Tangerang and Malang seems to be almost similar, while that of South Jakarta lies below them. This suggests that in general, the area having more dense BTSs gives less standard

deviation. The aggregate standard deviation supports this suggestion (see the graph in Figure 10). Another interesting finding is that the standard deviations of the three testbeds tend to converge when the number of reported towers increases (refer again to Tables 3 to 5 and Figures 9(a) to 9(c)).

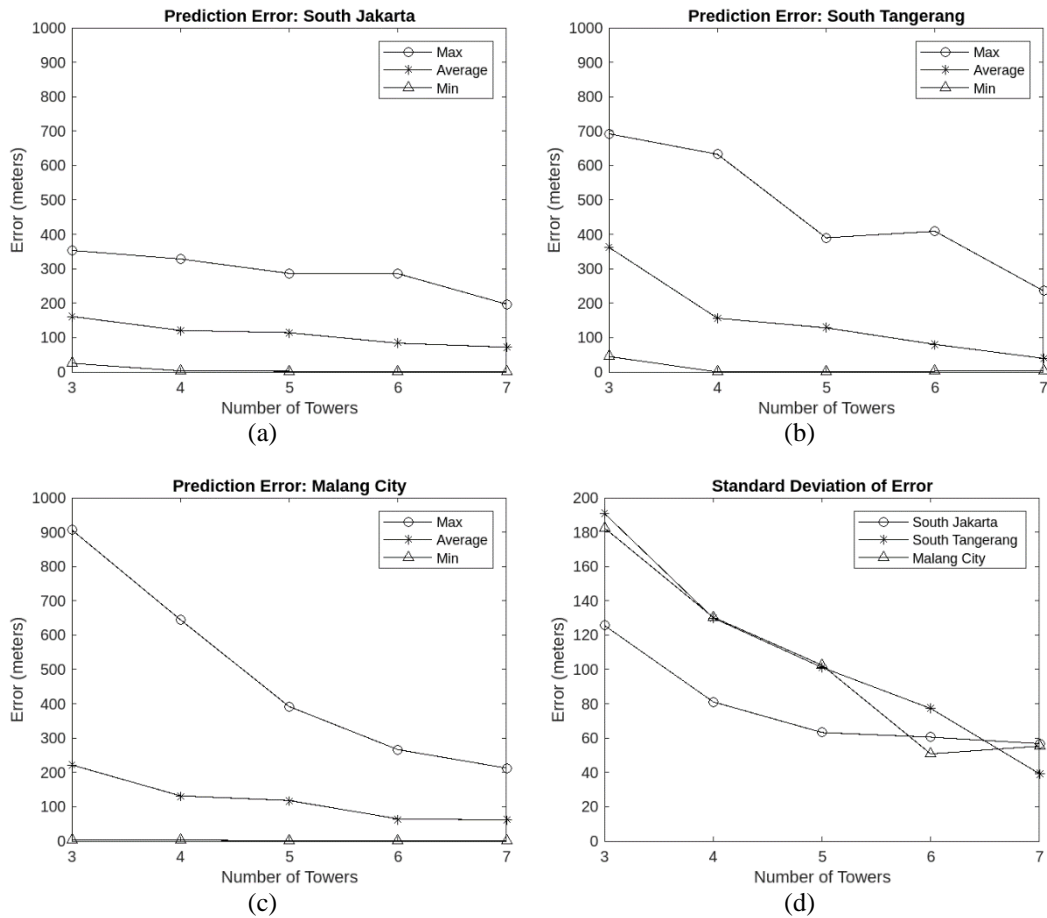


Figure 9. Range of error concerning the number of reported towers in (a) South Jakarta, (b) South Tangerang, (c) Malang City, and (d) standard deviation of error in each city

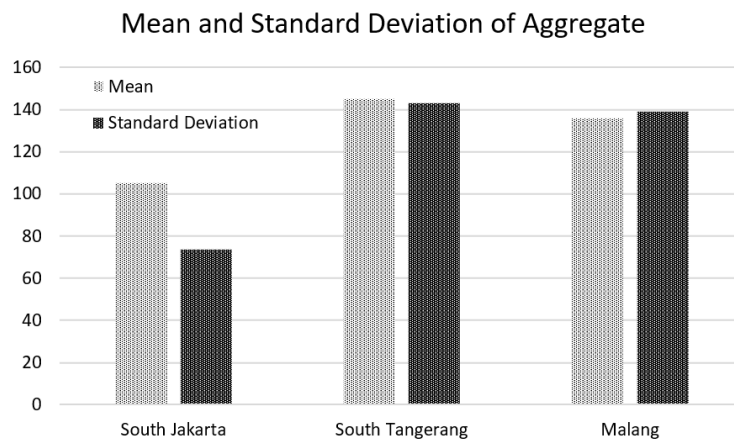


Figure 10. Aggregate mean and standard deviation of error in each testbed. More dense BTSs decrease errors (as shown by the results of South Jakarta testbed)

In terms of the number of reported towers, their distributions approximate a normal curve with a median of 5 for all testbeds. This is coherent with our previous finding that the CDFs of 5 towers are close to those of the aggregates as shown in Figure 11. Table 6 gives the resume of the results from merged testbeds, based on the smallest prediction error of each metric. The resume shows that three of the four best results are given by 7 Towers involvement, and also three of the four best results are from the South Tangerang testbed. The resume suggests that better results are likely achieved when there are more towers involved within the region having a lot of open space. For comparison, here we give the test results from other research in their testbed: i) Relative received signal strength [6]: 29 m mean error (Cairo, Egypt); ii) CellSense [7]: 30 m median (Cairo, Egypt); iii) Bayesian [7]: 52.8 m mean error (Tokyo, Japan); and iv) Pearson coefficient correlation [8]: 80% of error is below 300 (unmentioned location).

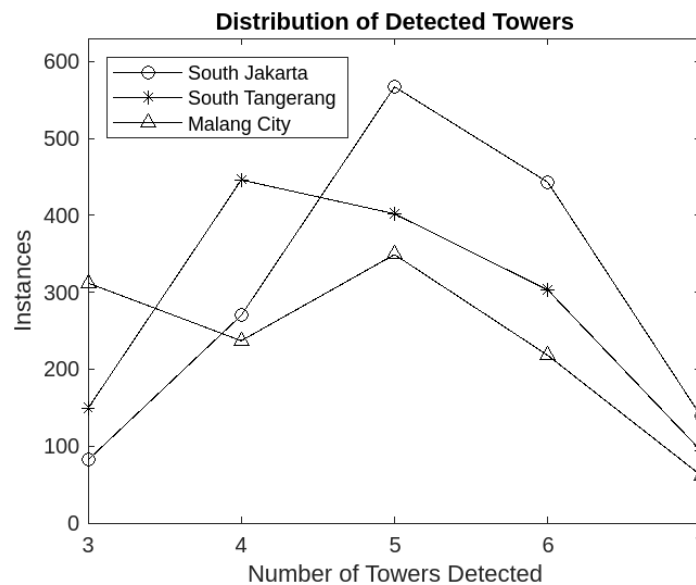


Figure 11. Distribution of reported towers among testbeds

Table 6. The smallest prediction error in each metrics

Metric	The best result (meters)	The testbed and the number of reported towers
Average	39.60	South Tangerang, 7 towers
Maximum	197.08	South Jakarta, 7 towers
Minimum	0.05	South Tangerang, 4 towers
Standard deviation	39.22	South Tangerang, 7 towers

4. CONCLUSION

This research presents an optimization model for the prediction of mobile device location using NMR and fingerprinting techniques. The proposed method demonstrates a notable level of accuracy in comparison to other prominent methods. The present research yields several consistent patterns that have been observed in our findings. Generally, a greater number of reported towers corresponds to a narrower range of error predictions, as well as a lower average and standard deviation of errors. The stability and consistency of error predictions, error average, and standard deviation increase as the density of BTSs in each observed area increases. The observed distribution of reported towers tends to approximate a normal distribution. By considering a range of 3 to 7 reported towers, the CDF of the aggregate tends to approach the CDF of 5 reported towers.




ACKNOWLEDGEMENTS

We would like to thank to Directorate of Research and Community Service, Ministry of Education, Culture, Research and Technology, Republic of Indonesia (*DRPM Kemdikbud dan Ristek Republik Indonesia*) for financing the research by Grant No. 069/E5/PG.02.00.PT/2022.




REFERENCES

- [1] R. Yamamoto, H. Matsutani, H. Matsuki, T. Oono, and H. Ohtsuka, "Position location technologies using signal strength in cellular systems," in *IEEE Vehicular Technology Conference*, 2001, pp. 2570–2574. doi: 10.1109/vetecs.2001.944065.
- [2] J. Martinka, "Locating mobile phones using signal strength measurements," Masaryk University, 2019.
- [3] H. Liu, Y. Zhang, X. Su, X. Li, and N. Xu, "Mobile localization based on received signal strength and Pearson's correlation coefficient," *International Journal of Distributed Sensor Networks*, pp. 1–10, 2015, doi: 10.1155/2015/157046.
- [4] R. Haeb-Umbach and S. Peschke, "A novel similarity measure for positioning cellular phones by a comparison with a database of signal power levels," *IEEE Transactions on Vehicular Technology*, vol. 56, no. 1, pp. 368–372, 2007, doi: 10.1109/TVT.2006.889563.
- [5] M. Ibrahim and M. Youssef, "CellSense: an accurate energy-efficient GSM positioning system," *IEEE Transactions on Vehicular Technology*, vol. 61, no. 1, pp. 286–296, 2012, doi: 10.1109/TVT.2011.2173771.
- [6] R. Elbakly and M. Youssef, "Crescendo: aAn Infrastructure-free ubiquitous cellular network-based localization system," in *2019 IEEE Wireless Communications and Networking Conference (WCNC)*, IEEE, Apr. 2019, pp. 1–6. doi: 10.1109/WCNC.2019.8885420.
- [7] M. H. A. Meniem, A. M. Hamad, and E. Shaaban, "GSM-based positioning technique using relative received signal strength," *International Journal of Handheld Computing Research*, vol. 4, no. 4, pp. 38–51, Oct. 2013, doi: 10.4018/ijhcr.2013100103.
- [8] S. A. Hussain *et al.*, "Positioning a mobile subscriber in a cellular network," *IAENG International Journal of Computer Science*, vol. 34, no. 2, pp. 1–6, 2007.
- [9] R. Kosasih and A. Sabri, "Predicting the location of a mobile device using weighted centroid method," *AIP Conference Proceedings*, vol. 2689, no. 1, pp. 1–7, 2023, doi: 10.1063/5.0114441.
- [10] Alnahari *et al.*, "Modified weighted centroid algorithm for indoor and outdoor positioning using wireless sensors network," *International Journal of Advanced and Applied Sciences*, vol. 5, no. 2, pp. 33–36, Feb. 2018, doi: 10.21833/ijaas.2018.02.006.
- [11] R. D. Ainul, "Enhancement of weighted centroid algorithm for indoor mobile non-cooperative localization system," in *International Conference on Informatics, Technology, and Engineering*, 2020, pp. 20–25.
- [12] J. Tang and J. Han, "An improved received signal strength indicator positioning algorithm based on weighted centroid and adaptive threshold selection," *Alexandria Engineering Journal*, vol. 60, no. 4, pp. 3915–3920, 2021, doi: 10.1016/j.aej.2021.02.031.
- [13] M. K. Goonjur, I. D. Sumitra, and S. Supatmi, "Enhanced the weighted centroid localization algorithm based on received strength signal in indoor wireless sensor network," *International Journal of Informatics, Information System and Computer Engineering (INJIISCOM)*, vol. 1, no. 1, pp. 13–22, 2020, doi: 10.34010/injiiscom.v1i1.4016.
- [14] R. Kosasih and A. Sabri, "Mobile device positioning by using dynamic weighted centroid model," in *2022 7th International Conference on Informatics and Computing, ICIC 2022*, IEEE, 2022, pp. 7–10. doi: 10.1109/ICIC56845.2022.10006962.
- [15] L. S. Ezema and C. I. Ani, "Multi linear regression model for mobile location estimation in GSM network," *Indian Journal of Science and Technology*, vol. 9, no. 6, pp. 1–6, 2016, doi: 10.17485/ijst/2016/v9i6/75195.
- [16] D. B. Lin and R. T. Juang, "Mobile location estimation based on differences of signal attenuations for GSM systems," *IEEE Transactions on Vehicular Technology*, vol. 54, no. 4, pp. 1447–1454, 2005, doi: 10.1109/TVT.2005.851318.
- [17] L. Jarvis, J. McEachen, and H. Loomis, "Geolocation of LTE subscriber stations based on the timing advance ranging parameter," in *Proceedings - IEEE Military Communications Conference MILCOM*, 2011, pp. 180–187. doi: 10.1109/MILCOM.2011.6127575.
- [18] Z. Shakir, J. Zec, and I. Kostanic, "Position location based on measurement reports in LTE cellular networks," in *2018 IEEE 19th Wireless and Microwave Technology Conference, WAMICON 2018*, IEEE, 2018, pp. 1–6. doi: 10.1109/WAMICON.2018.8363501.
- [19] A. Varshavsky, E. de Lara, J. Hightower, A. LaMarca, and V. Otsason, "GSM indoor localization," *Pervasive and Mobile Computing*, vol. 3, no. 6, pp. 698–720, 2007, doi: 10.1016/j.pmcj.2007.07.004.
- [20] F. Shang, W. Su, Q. Wang, H. Gao, and Q. Fu, "A location estimation algorithm based on RSSI vector similarity degree," *International Journal of Distributed Sensor Networks*, pp. 1–22, 2014, doi: 10.1155/2014/371350.
- [21] O. G. Esenbuga, "Comparison of principal geodetic distance calculation methods for automated province assignment in Turkey," *16th International Multidisciplinary Scientific GeoConference SGEM2016, Informatics, Geoinformatics and Remote Sensing*, vol. 2, pp. 141–148, 2016, doi: 10.5593/sgem2016/b22/s09.019.
- [22] J. P. Gomes, J. P. Sousa, C. R. Cunha, and E. P. Morais, "An indoor navigation architecture using variable data sources for blind and visually impaired persons," *Iberian Conference on Information Systems and Technologies, CISTI*, pp. 1–5, 2018, doi: 10.23919/CISTI.2018.8399347.
- [23] B. Xu, "Research on indoor environment positioning system considering multisensor in the multi-information data fusion," *Mobile Information Systems*, pp. 1–10, 2022, doi: 10.1155/2022/1676155.
- [24] A. Sabri and R. Kosasih, "An optimization model for network-based mobile positioning," in *2021 15th International Conference on Advanced Computing and Applications (ACOMP)*, IEEE, Nov. 2021, pp. 191–195. doi: 10.1109/ACOMP53746.2021.00034.
- [25] K. Gade, "A non-singular horizontal position representation," *Journal of Navigation*, vol. 63, no. 3, pp. 395–417, 2010, doi: 10.1017/S0373463309990415.
- [26] R. A. Azdy and F. Darnis, "Use of haversine formula in finding distance between temporary shelter and waste end processing sites," *Journal of Physics: Conference Series*, vol. 1500, no. 1, pp. 1–7, 2020, doi: 10.1088/1742-6596/1500/1/012104.
- [27] M. Basyir, M. Nasir, S. Suryati, and W. Mellyssa, "Determination of nearest emergency service office using haversine formula based on android platform," *EMITTER International Journal of Engineering Technology*, vol. 5, no. 2, pp. 270–278, 2018, doi: 10.24003/emitter.v5i2.220.
- [28] Q. Wang *et al.*, "Recent advances in floor positioning based on smartphone," *Measurement: Journal of the International Measurement Confederation*, vol. 214, 2023, doi: 10.1016/j.measurement.2023.112813.

BIOGRAPHIES OF AUTHORS

Ahmad Sabri    received a B.Sc. degree in mathematics from the University of Indonesia in 1997, and his M.Sc. in mathematics from the University of Indonesia in 2011. He received his doctoral degree in informatics from Université de Bourgogne, Dijon, France, in 2015, under a doctoral scholarship from the Government of Indonesia. He currently works as a lecturer and researcher in the Department of Informatics, at Gunadarma University, Jakarta, Indonesia. His research interests are enumerative combinatorics, machine learning, and mobile positioning. He can be contacted at email: sabri@staff.gunadarma.ac.id.



Rifki Kosasih    received a B.Sc. degree in mathematics from the University of Indonesia in 2009, an M.Sc. degree in mathematics from the University of Indonesia in 2012, and a Ph.D. degree in information technology from Gunadarma University, Indonesia, in 2015. He is now a lecturer and researcher in the Department of Informatics, at Gunadarma University, Jakarta, Indonesia. His research interests are image processing, object recognition, data science, manifold learning, machine learning, mobile positioning, and deep learning. He can be contacted at email: rifki_kosasih@staff.gunadarma.ac.id.